

**K. Haga, Y.L. Wang, H. Oshita, M. Nomura
K. Hirano, S. Tōyama, N. Takahashi, T. Emoto, Y. Himeno**

**Power Reactor and Nuclear Fuel Development Corporation
Oarai Engineering Center
4002 Narita, Oarai-Machi, Ibaraki, 311-13, Japan**

L Sato

**National Laboratory for High Energy Physics
1-1 Oho, Tukuba, Ibaraki, 305, Japan**

Abstract

In PNC(Power Reactor and Nuclear Fuel Development Corporation), a research and development (R&D) for a high-power CW electron linac is in progress. The present target of the R&D is to demonstrate the technological feasibility of a high power electron linac whose beam current is, maximum 100 mA and average 20 mA at the energy level of 10 MeV. This linac is expected to lead more a powerful demonstration one that can be used as a transmutation system for fission products.

Basic configuration of the high power is an accelerator tube with TWRR(Traveling Wave Resonant Ring), RF source with klystrons, and a injection system. The test model of an accelerator with TWRR and a klystron have been fabricated and were subjected to experiment. Those models were assembled in one test apparatus in KEK and their RF power testis being conducted.

Recently, developments of electron gun, chopper, and buncher in the injection system have been started.. The electron gun is required to emit a current of about 400 mA and emittance must be as low as possible. Survey of previous studies and analysis on electron trajectory by the EGUN code conducted by the present authors concluded that a DC gun using Ba impregnated dispenser cathode is most preferable to the first usage in the linac system. As for the buncher, a constant gradient structure with TWRR is chosen and the detail design and the trial manufacturing will start soon.

The construction of the whole linac system is scheduled to initiate from fiscal year 1993. The first beam is scheduled in 1996 after the preceding test of injection system in the previous year.

1 Introduction

It is often mentioned that accelerator is one of the promising tools to transmute fission products which have small neutron capture cross sections such as Sr-90 and CS-137. However, no such a high current CW (Continuous Wave) accelerator does not exist in the world as to be able to use to that purpose in an engineering scale. PNC started a high power accelerator development project. Electron linac was chosen in this project because a clean transmutation process is expected by the gamma-neutron reaction. Its key components development has been conducted since 1988.

The objective of present research and development (R&D) is to prove technical capability to construct a high current electron linac whose beam current is maximum 100 mA and average 20 mA at the energy of 10 MeV [1]. Target specifications and schematic of the system are shown in Table 1 and Fig.1, respectively. The basic configuration of accelerator tube of this high-power electron linac is adoption of TWRR (traveling wave resonant ring). Test components of an accelerator tube with TWRR and a klystron have been fabricated and assembled in KEK (National Laboratory for High Energy Physics) and RF power tests are in progress [2]. The design study of injection system including electron gun, chopper, and buncher started this year. This work will be followed by the trial manufacture.

Besides the recent progress of R&Ds on these important elements, the paper presents future plan including construction schedule of the linac.

2 Concept of Design

The basic design of this accelerator was performed based on the following principles to overcome the technical problems related to the high intensity beam and the high quality beam[3].

(i) High current threshold to beam break-up:

Adoption of $2\pi/3$ mode, L-band frequency

Constant gradient structure under 100 mA condition

Short length accelerator tube (1.2 m) with a small attenuation structure

(ii) High efficiency

Attachment of TWRR to each accelerator tube

(iii) Narrow energy spread and narrow phase width and low beam emittance:

Low emittance electron gun

Chopper-prebuncher operation

Linearly-tapered phase velocity buncher with TWRR

(iv) Prevention of thermal deformation caused by RF loss:

Increase of accelerator efficiency

internal cooling water structure

3 Key Components Element Development

There are many technical problems to be solved to fulfill the target specifications of this accelerator system. Among them our main achievements in the key components are described here.

..

3-1 Accelerator tube[4]

The accelerating part consists of eight accelerating sections one is the buncher in the injection system and other seven regular tube after the injection system. Each section whose length is 1.2m contains fifteen $2\pi/3$ mode cavities including two coupling cavities. Those cavities are designed to have a constant gradient structure under the condition of 100 mA beam loading. According to the progressive stop-band technique, the iris diameters in the initial region of the regular section are smaller than those in any preceding ones but larger than those in subsequently located ones. The purpose is to enhance the threshold current of the beam break-up (BBU). In Fig. 2 the wave phase velocity, iris diameters and accelerating field of the buncher and two types of regular tube structures are shown.

Using the short accelerating sections and low attenuation structures, not only increase the threshold current of BBU, but also release the tolerances of the frequency, temperature and fabrication. But in this case, it will result in low electric field throughout. Therefore, we use traveling wave resonant ring (TWRR) to improve its efficiency.

Each TWRR includes one regular tube, phase shifter, and stub tuner. One may use

the phase shifter to make the TWRR resonance, and the stub tuner to match TWRR. . . After tuning and matching, the multiplication factor M becomes maximum.

Design calculation revealed that the multiplication factor M of the present TWRR is about 2 and 3 for accelerator tube with and without beam loading respectively. It means that the electric field in the accelerator tube is 2 or 3 times higher than without TWRR.

In general, cooling design is one of the important issue for a high power accelerator because of its large heat generation. The accelerator cooling structure of the present accelerator tube is designed as shown in Fig.3. The cooling water passes through eight flow paths provided in the wall of the accelerator and the disks. According to the three-dimensional finite-element heat transfer and thermal stress analysis, enough cooling capacity can be obtained without causing thermal deformation for one accelerator tube under 20% duty factor.

3-2 Klystron

The target specifications of a high-power CW klystron under development are listed in Table2.

After the successful operation of the first prototype klystron in pulse operation (with pulse width: 15 μ s, peak-power: 1200 kW, efficiency 63%), the second prototype klystron was fabricated in 1991, then its preliminary high-power test was carried out at the manufacturer (Toshiba Corporation, Nasu Works). A maximum peak power of 780 kW with an efficiency of 46% has been obtained at a beam voltage of 85 kV, a beam current of 20 A in 50 ms pulse operation.

This tube is presently under high-power testing at TRISTAN klystron test bench in KEK. Currently, the tube produced 330kW CW RF output with an efficiency of 31% at a beam voltage of 75kV and a beam current of 14A, which are the present limits under the CW operation due to the overheating of the RF vacuum window. However this RF power is enough to test one accelerator tube with the TWRR, whose details are mentioned in the chapter 3-5 of the present paper.

Since 1200 kW and 63% at 90 kV using a short pulse and 780 kW using long pulse had already been obtained using test tubes, the only problem we encountered is non-uniform over heating of the RF vacuum window. The window fails due to the thermal stresses generated by the unequal temperature distribution across the window surface by dielectric losses and flash over such as multipactoring. To solve this problem, the

high power RF prototype windows are being designed and fabricated to get practical experience by conducting a window RF test separately. In the design, the dielectric losses, the strength of electric field in the window cavity (π I I -box) is intended to be reduced by optimizing the dimension of the window cavity. Beryllia was chosen as the material of the prototype klystron window, however high-purity alumina, aluminum nitride, and carbon nitride are also promising candidates. Therefore, they will be used for windows in the coming the testing using the TWRR.

3-3 Klystron RF Control System

Function of the klystron RF control system is to maintain the klystron beam current, amplitude and phase for proper operation of the klystron for the high power RF accelerator tube test. Fig. 4 shows its schematic diagram at the KEK test bench. The main components of the RF control system are 1) a klystron driver, 2) a klystron anode controller, 3) feedback system, and 4) an interlock controller. In the system, the RF signal from a signal generator is divided into two RF signals that run the driver amplifier for the klystron and the reference signal to a local oscillator. The klystron anode controller manages to avoid power dissipation and protect over heating at the klystron collector. The beam current is controlled as a function of the required output power of the klystron. The linearly detected RF amplitude of the driver power is fed into the function generator. The modulation anode voltage controlled by the functions mentioned above gives a proper beam current to avoid the over load or over collector heating in the klystron at any required output power. The RF signals picked up at the directional coupler near the klystron are linearly detected and then compared with the reference voltage. The difference of these two signals is fed to control the RF driver power of the klystron through the feedback controller.

To examine the performance of the system shown in Table. 2, test was carried out. The obtained stability of amplitude was within $\pm 1\%$. The phase signals picked up at the directional coupler near the resonant ring were locked to the reference line phase by converting to 1 MHz IF signals as shown in Fig. 4. The phase detection system worked within ± 1 degree error for input power levels of 300 kW.

The interlocks employed in the low level RF control system are two groups characterized by the response speed. Fast interlocks consist of the fast signals such as RF reflection and arc detector attached at the klystron output window, which works

within an order of micro-second to switch ~~off~~ the drive RF signals. The normal interlocks are for the resonant ring cooling water flow, vacuum of the resonant ring, and the temperature of these items.

3-4 Injector System

The following design features were adopted for the injection system to obtain a narrow energy spread ($\pm 0.2\%$) and a low beam emittance (5π mm mrad):

- (i) use of a 200 kV electron gun with a cathode of small radius (4mm);
- (ii) strict avoidance of a gridded electron gun and of any beam intercepting control or monitoring elements;
- (iii) concentration of design effort on attaining a laminar beam of long focal length and small cross-section;
- (iv) use of a ~~do~~ magnetically biased transverse deflection chopper cavity arranged so that the beam transmission occurs paraxial with center line;
- (v) use of a low prebunching parameter 200 ± 15 kV modulation;
- (vi) the prebuncher and buncher are designed so as to avoid phase orbit cross-overs as much as possible.

To realize the above features, a basic configuration of the injection system was decided to consist of a 200 kV electron gun, an RF chopper-prebuncher drift space assembly, a tapered phase velocity buncher 1.2 meter long and a 1.2 meter velocity-of-light pre-accelerator section as shown on the left part of Fig.1.

The chopper is a phase gate which consists of an RF deflecting cavity and clipping aperture to select a beam bunch from the gun during 90° of the each RF cycle.

The prebuncher is to bunch beam less than 10^{-6} by velocity modulation. Its cavity is located ahead of the chopper clipping aperture to avoid phase shifts due to the beam loading, and it is possible to prevent an additional RF power being induced in the cavity by the chopped beam and this enables the gap voltage to be selected by simple adjustment of the drive line attenuation.

The calculated design outline is described as follows. The beam is bunched less than 3^{-6} with energy 1.9 MeV during the buncher. During the pre-accelerator section the beam keeps its bunching width and accelerate to 3.6 MeV.

In the injection system, in addition to the longitudinal compression as stated above, the beam will be compressed radially by the thin lenses, solenoids and Q magnets.

There are beam monitors and steering coils in X and Y directions to keep the beam on the axis.

3.4.1 Electron gun

Many kinds of materials are used for the cathode of an electron gun, i.e. pure metal, oxide, impregnated dispenser materials (Ba cathode) and LaB₆. Each material has some advantages and disadvantages. For example, a pure metal cathode cannot achieve a high current density. LaB₆ cathode can achieve a high current density, but this is unstable and has a short life time. Oxide cathode and Ba cathode can achieve a high current density. Furthermore, these cathodes are stable and are very popular for an electron gun. From the viewpoints of stability and current density, we selected a Ba cathode. Its weak point is that the lifetime is unknown in CW and high current conditions. Therefore, its test is planned.

Concerning the accelerating field, a higher gradient field is favorable since electron beams are subject to space-charge forces that lead to emittance growth. At low energy, in general, fields obtained in an RF cavity are higher than DC fields. But from the present emittance requirement of this linac, DC fields are sufficient for our electron gun. But if a lower emittance is required, an RF field will be necessary. We tentatively selected a DC field.

The electron trajectory in the electron gun is calculated by EGUN code [5]. A preliminary result is shown in Fig. 5. It can be seen that the beam radius is kept small.

3+2, Chopper [6]

The rectangular chopper cavity that is to be designed to be operated with the TE₁₀₂ mode sweeps the beam across the clipping aperture located in the tungsten block assembly at a frequency of 1249.135 MHz. By using a DC magnetic bias at the chopper cavity, the beam scan is offset to one side of the system center line and the 90° of each RF cycle transmits through the clipping aperture.

The beam is arranged to sweep along a water-cooled V-shaped notch which is cut in

the incident surface of the tungsten block to reduce the dissipation per unit area and to avoid surface erosion.

The chopper cavity will be made of oxygen-free high- conductivity copper(OFHC) and requires about few hundreds-watt of RF power (unloaded Q of 10000). The cavity is watercooled and the temperature is controlled within on accuracy of $\pm 0.1^{\circ}\text{C}$ for target value.

343, Prebuncher

The output phase width from the prebuncher $\Delta\phi_{out} = 7^{\circ}$ is chosen by following discussion. The prebuncher cavity resonates in the normal TM010 mode. In the buncher the phase relationship is defined by

$$\Delta\phi_{out} = \Delta\phi_{in} + \frac{2\pi L}{\lambda \beta_e} \left(1 - \frac{\beta_{e0}}{\beta_e} \right)$$

where β_{e0} and β_e are electron velocities for input and output respectively,

$$\beta_{e0} = \sqrt{1 - \frac{(m_0 c^2)^2}{(m_0 c^2 + eV_0)^2}}$$

$$\beta_e = \sqrt{1 - \frac{(m_0 c^2)^2}{(m_0 c^2 + eV_0 + eV_g \sin \Phi_{in})^2}}$$

When we choose $\lambda = 0.24\text{m}$, $V_0 = 200 \text{ kV}$, $\beta_{e0} = 0.695c$, $L = 1.2\text{m}$ and $V_g = 15 \text{ kV}$, $\Delta\phi_{in} = 90^{\circ}$ from previous chapter, we can get $\Delta\phi_{out} = 7^{\circ}$.

345, **Buncher**

The buncher section employs a $2\pi/3$ mode traveling wave type. In designing the buncher section, emphasis was placed on:

- (i) to avoid the phase orbit crossovers as much as possible to obtain a narrow energy spread and a small bunch width. In the buncher, the wave phase velocity varies linearly and slowly, at the first half part from $0.695c$ to $0.930c$ and in the second half from $0.930c$ to $0.99c$.
- (ii) to avoid uniform power dissipation to bring about thermal phase variations. The structure is designed so as to have a constant gradient of power dissipation under beam loading condition.
- (iii) to minimize transverse momenta contributions to the beam. The input and output coupling cavities are designed with offset cavities to symmetrize the RF fields.

3.4 RF power test

The RF power test that is consisted of low and high power tests was performed to examine the RF characteristics of the test accelerator tube with TWRR i.e. field multiplication factor M , standing wave ratio VSWR and quality factor Q value.

The low power test is executed by injecting slight RF from a network analyzer into the TWRR. The test results are shown in Table 1. The best value of M was 2.9 and, most of case, around 2.6 depending on conditions.

After the low power test, the high power test was performed by connecting the TWRR with the klystron. Fig. 6 shows an arrangement of the high power test apparatus. The RF high power from the klystron was equally divided into two paths by magic-tee. One path reached a dummy load through a stub tuner and the other went through a long straight wave guide to the TWRR. The high power test had three objectives. First one was to certify whether the results of the low power test in the high power test. Second one was to check the capability of the coolant system whose details were presented in chapter 3-1 so as not to change the RF characteristics of the test apparatus by some thermal expansion. Third one was to find out unpredictable' problems generated injecting of high power. The present state of the high power test is as follows. The maximum operation RF power was limited by about 28kW from the klystron(or ~83kW

in the TWRR). After adjusting the frequency to make TWRR resonance, measured multiplication factor was 2.6 that was close to the value measured in the low power test.

4 Future Plan

Fig. 7 shows a future PNC's plan of the electron linac development. After RF power test using prototype klystron and accelerator tube presented, a prototype injection system will be designed and manufactured and it will be subjected to performance test from 1993.

The main item of this plan is the construction of the whole linac system whose total length is about 20 m. It is scheduled to get the first beam in 1996 after the preceding test of the injection system in the previous year.

Even after the design and construction of the first-stage accelerator are commenced, key components development will be continued seeking for modification to realize higher energy and higher quality beam in this accelerator. Higher duty factor more than 20% will be also another technical target of this project.

5 Summary

R&D has been continued to develop a high-power CW electron linac in PNC. The present target specifications of the linac is maximum 100 mA and average 20 mA at the beam energy of 10 MeV.

The crucially important points of this linac are the effectiveness of TWRR and the availability of elements in the injection system including electron gun. The former seems to have been proved from RF tests. On the other hand, the research of injection system began this year and more efforts are needed in this field.

Based on the R&D of key components so far, although there are so many things left, for example, control system development and designing of exhaust gas treatment system, a tentative construction schedule has been drawn. The first operation is scheduled in 1996 after the preceding test of injection section in the previous year.

Acknowledgments

This project is being performed under the guidance of professors of KEK. Among them the authors should express their special thanks to M. One, A. Enomoto and S. Yoshimoto for their help in the RF test performed in KEK. The authors should remember the administrative contribution of M. Sakuma to this project.

References

1. Y. Himeno et al., "Development of Ultra-High Power Electron Linac Accelerator," PNC Report TN941 091-337, March 1992.
2. L Sato et al., "Development of a CW Electron Linac Structure Using a Traveling-Wave Resonant Ring," Third European Particle Accelerator Conference, Berlin, March 24-25,1992.
(KEK Preprint 92-13, April 1992)
3. Y.L. Wang et al., "Design Study of PNC Super Power Electron Linac," under submission to J. Nuclear Science and Technology.
4. Y.L. Wang and L Sate, "Study of Characteristics of Traveling Wave Resonant Ring for High Power CW Electron Linear Accelerator," Proc. of the 19th Linear Accelerator Meeting in Japan, pp.100-102, Sendai, September 1-3,1992.
5. W.B. Herrmannsfeldt, "SLAC-226, Electron Trajectory Program," 1979.
6. J.Haimson, IEEE. Trans. on Nucl. Sci. NS-12 499, June 1965.
7. J. Haimson, "Injector and Waveguide Design Parameters for a High Energy Electron Linear Accelerator," IEEE Trans. Nucl. Sci. NS-12, 499, June 1965.

Table 1. Specification of CW linac

Energy	10 MeV
Beam Current	100 mA
Duty Factor	20%- 100%
Energy Spread	< $\pm 0.2\%$
Bunch Width	< 3 ''
Beam Emittance	5π mm mrad
Frequency	1249.135 MHz
Mode	$2\pi/3$
Structure	Constant Gradient Structure
Type	Traveling Wave Linac with TWRR

Table 2. Operating Condition

	typ.	
Frequency	1249	MHz
Heater voltage	12	v
Beam Voltage		
CW mode	90	kV
Pulse mode	147	kV
Beam Current		
CW mode	25	A
Pulse mode	65	A
Collector dissipation	800	kW

Table 3. RF characteristics of the TWRR(Low power test)

Temperature	Resonant frequency	Multiplication factor	VSWR	Q value
31 °C	1248.240 MHz	2.90-	1.03	10708
35°C	1248.139 MHz	2.83	1.09	10254
36-C	1248.114 MHz	2.62	---	9490

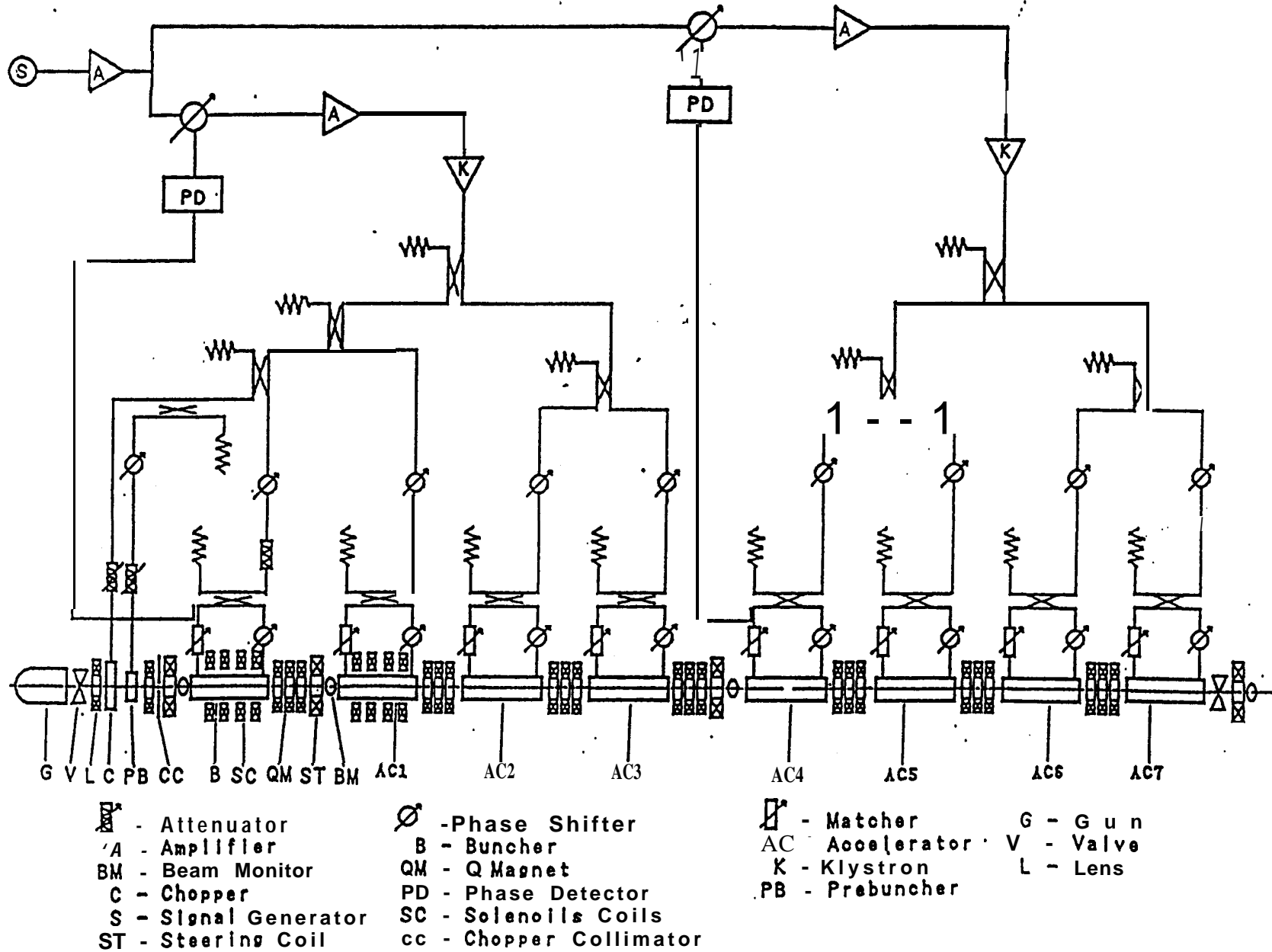


Fig.1 Schematic of CW Electron Linac

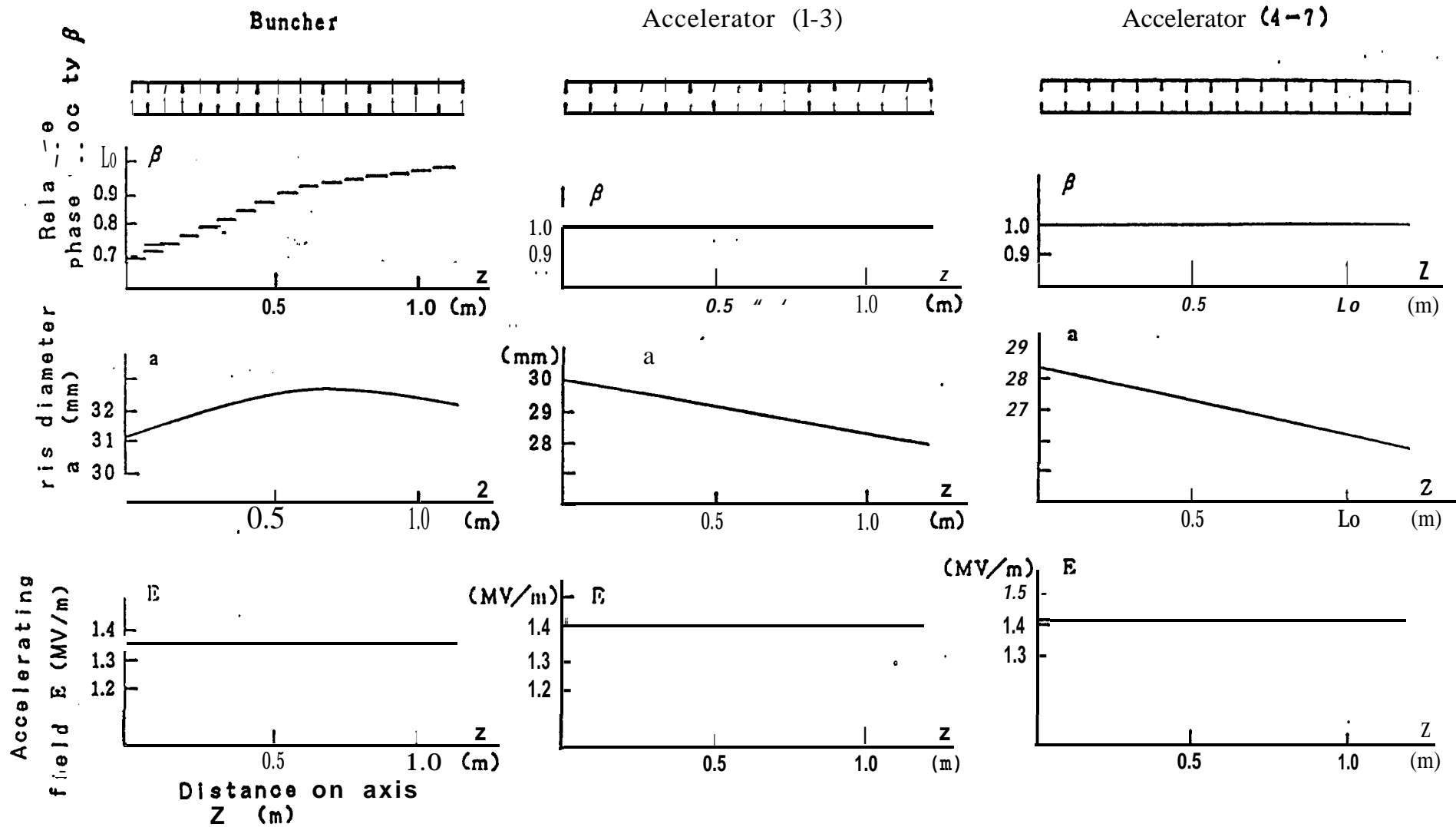
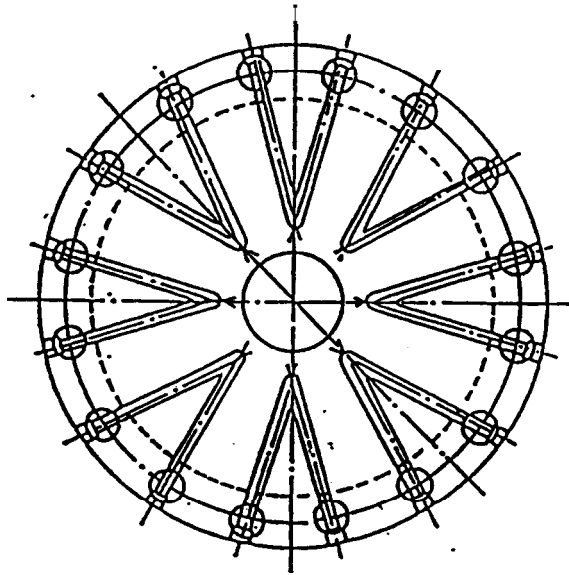


Fig. 2 Phase velocity, iris diameter, and accelerating field in the accelerator sections.



A - A cross section

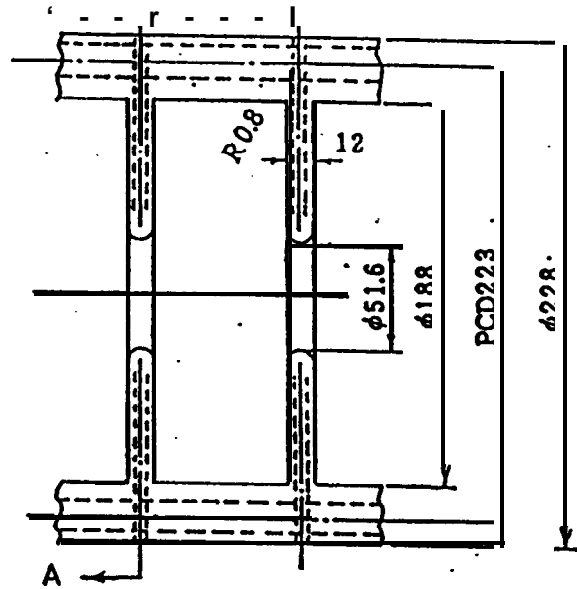


Fig.3 Accelerator internal cooling Structure .

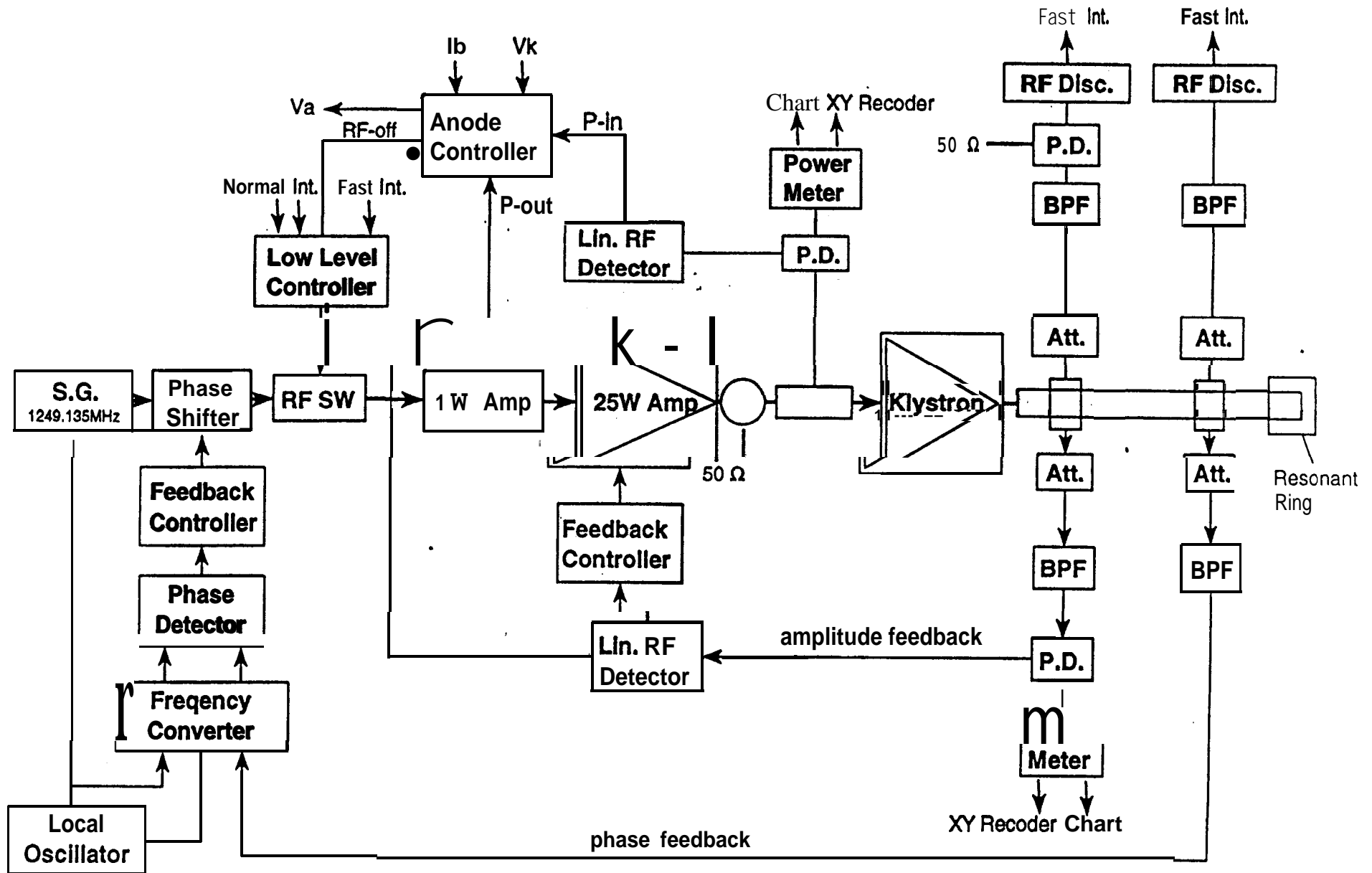


Fig. 4 RF Control System

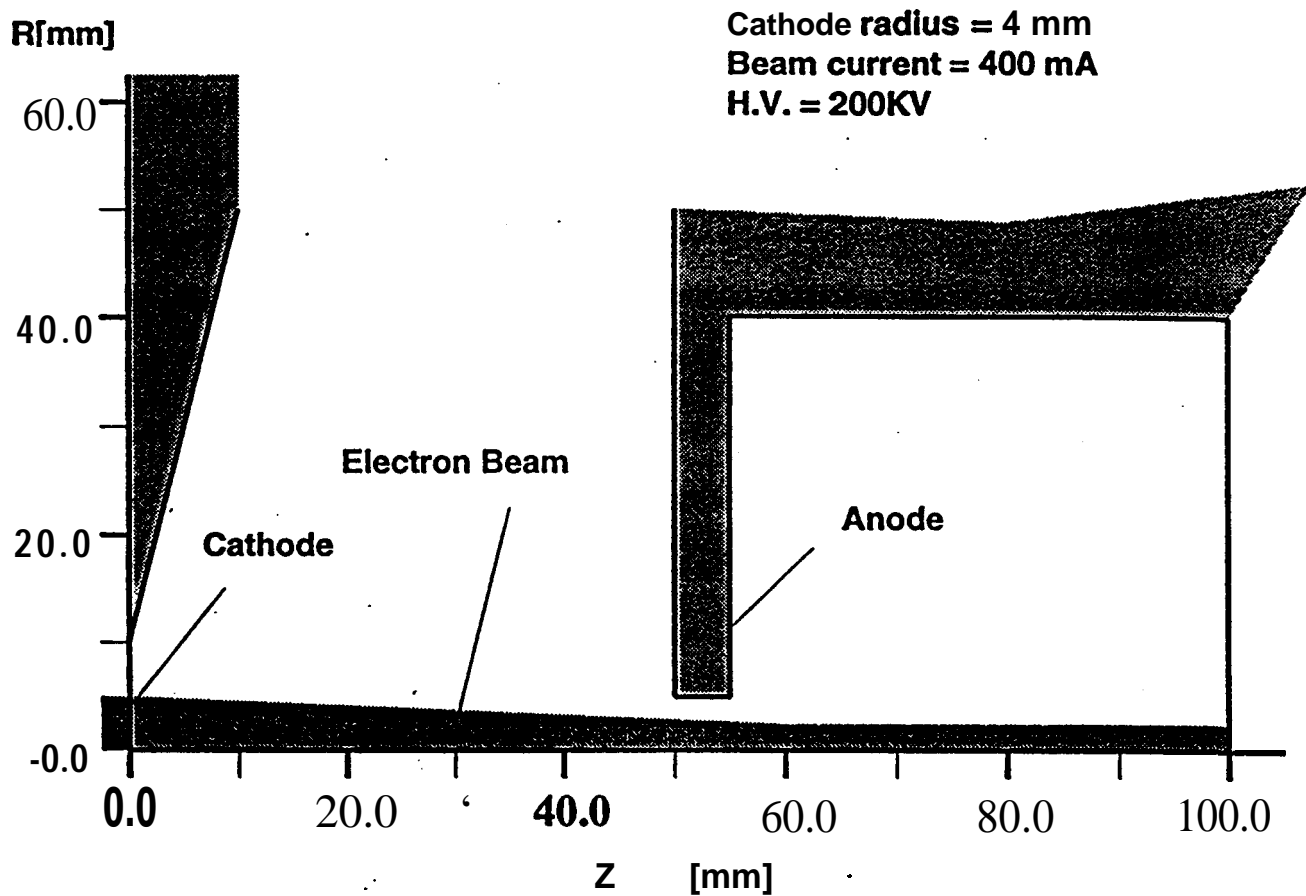


Fig. 5 Calculated electron trajectory

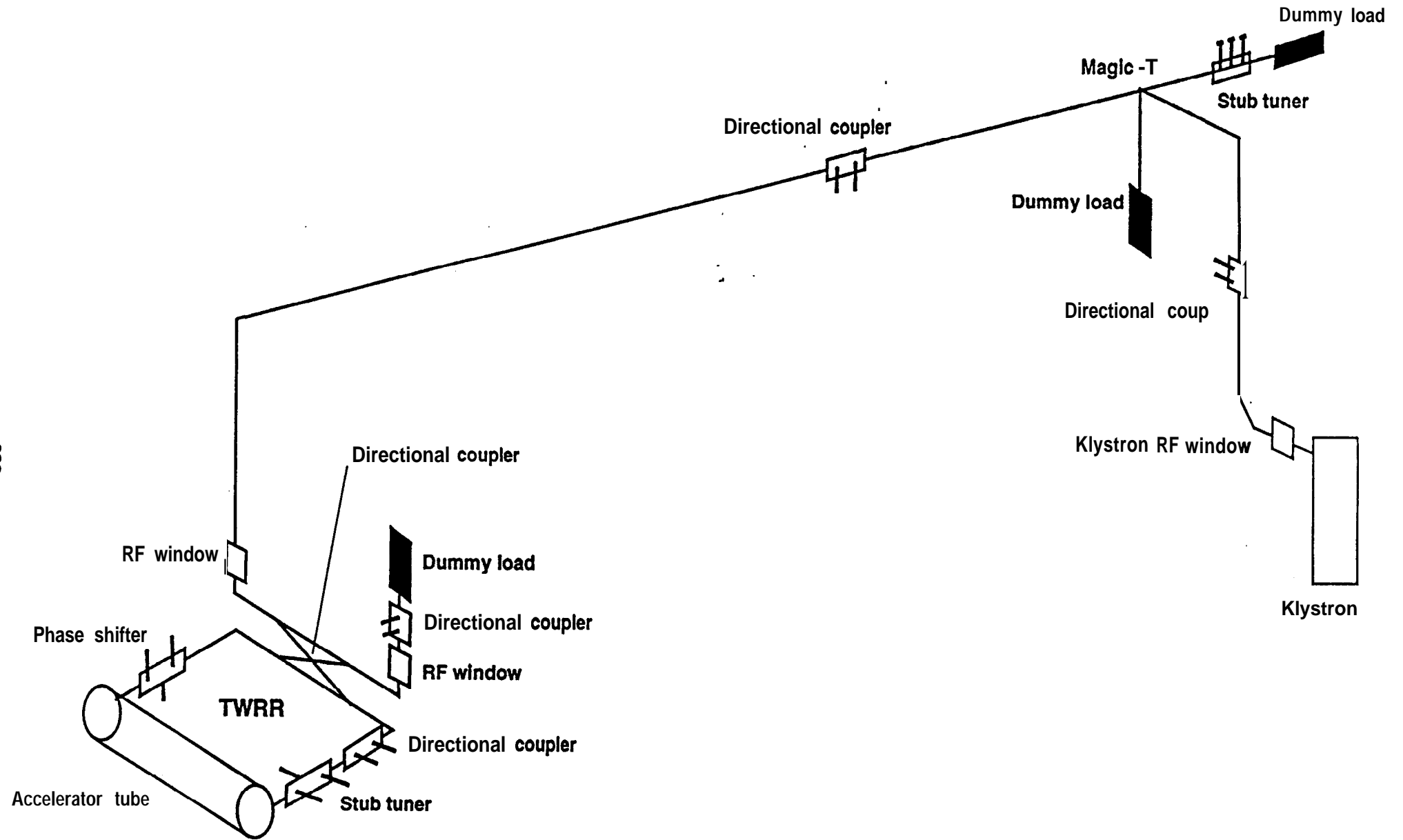


Fig. 6 The high power test apparatus

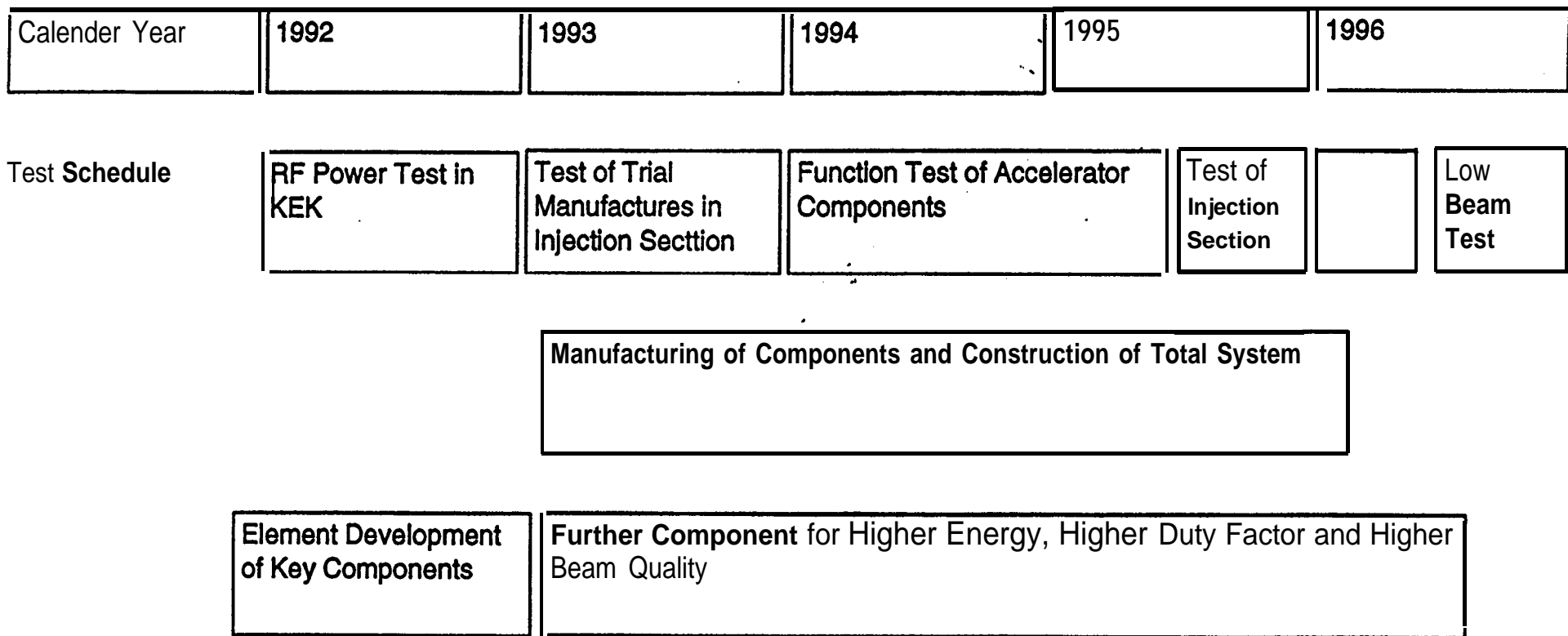


Fig. 7 Schedule of high power CW electron linac development